ISSN 0016-7029, Geochemistry International, 2021, Vol. 59, No. 4, pp. 413–421. © Pleiades Publishing, Ltd., 2021.
Russian Text © The Author(s), 2021, published in Geokhimiya, 2021, Vol. 66, No. 4, pp. 341–350.

Pleistocene Sediments of the Caribbean Sea

M. A. Levitan[a], *, T. A. Antonova[a], A. V. Kol'tsova[a], and K. V. Syromyatnikov[a]

[a] *Vernadsky Institute of Geochemistry and Analytical Chemistry, Russian Academy of Sciences, Moscow, 119991 Russia*

**e-mail: m-levitan@mail.ru*

Received March 12, 2020; revised September 1, 2020; accepted September 22, 2020

Abstract—The lithological-facies zoning of the Neo- and Eopleistocene sediments of the Caribbean Sea has been described for the first time based on deep-sea drilling data. Corresponding maps and isopach schemes were processed using A.B. Ronov's volumetric method to calculate the quantitative parameters of sedimentation for the distinguished types of Pleistocene sediments. It was revealed that the role of carbonate sediments increased from the east westward. The accumulation of lithogenic and carbonate planktic sediments was more intense in the Neopleistocene than in the Eopleistocene, which was related to the neotectonic orogeny on the Lesser Antilles.

Keywords: Caribbean Sea, Eopleistocene, Neopleistocene, areas, accumulation rate, carbonate sediments, terrigenous sediments

DOI: 10.1134/S0016702921040030

INTRODUCTION

This paper was made in the framework of a large project dedicated to the Pleistocene sediments of submarine margins of the World Ocean (Levitan et al., 2018, 2019, 2020, and others). This project considers separately Neopleistocene, i.e., Middle and Late Pleistocene (Q_{2+3}, roughly 0.01–0.80 Ma), and Eopleistocene or Early Pleistocene [Q_1, roughly 0.80–1.80 Ma according to the "old" scale (Gradstein et al., 2004)].

All the above-mentioned papers are organized according to the following scheme: (1) documentation of factual material with reference to the results of the corresponding deep-water drilling cruises; (2) description of the modern sedimentation environment in the studied basin; (3) characteristics of the main methods applied by the authors, e.g., comparative–lithological method by N.M. Strakhov (1945), volumetric method by A.B. Ronov (1949), facies analysis of oceanic sediments by I.O. Murdmaa (1987); (4) compilation of review lithological-facies maps with isopachs for the Neopleistocene and Eopleistocene age sections and their processing using volumetric method with calculation of quantitative parameters of sedimentation (area of mapped sediments, their volumes, mass of dry sediment, sediment accumulation rate per time unit); (5) discussion of obtained data and drawing the general conclusions.

It is known that the Atlantic Ocean is rimmed mainly by the passive-type continental margins. Active margins are the Caribbean and Scotia seas. The Pleistocene sedimentation in the Scotia Sea has been described by us previously (Levitan et al., 2020). This paper is focused on the Pleistocene deposits of the Caribbean Sea.

MODERN SEDIMENTATION ENVIRONMENTS

The Caribbean Sea located approximately between 9° and 22° N, 89° and 60° W represents a back-arc sedimentation basin. In the north, it is bordered by the Greater Antilles, which consist of an archipelago of large islands (Cuba, Haiti, Jamaica, and Puerto Rica). The Eastern and Southeastern limitations are the Lesser Antilles consisting of small Windward (in the east) and Leeward (in the southeast) islands. In the south and west, the Caribbean Sea is bounded by the South and Central America coast (Fig. 1). In the northwest, the Caribbean Sea through the Yucatan Strait is linked with the Gulf of Mexico. The area of the studied basin is 2753 thou. km^2 and its average depth is 2500 m (Sukhovei et al., 1980).

Being located in the tropical zone of the Northern Hemisphere, the Caribbean Sea has the high seasonal temperatures of the sea surface (from +23°C in the north to +27°C in the south in winter, and +28°C elsewhere in summer). The atmospheric circulation is controlled by trade winds (frequently replaced by tropical hurricanes in the northern part of the basin), while the surface currents are mainly of westerly and west-northwesterly (Guiana, Caribbean and Yucatan currents) (Fig. 1) (Sukhovei et al., 1980).

In general, the Caribbean Sea differs in the low primary production: its value usually accounts for less than 135 g C/m^2/yr. The deep Antarctic waters enriched in

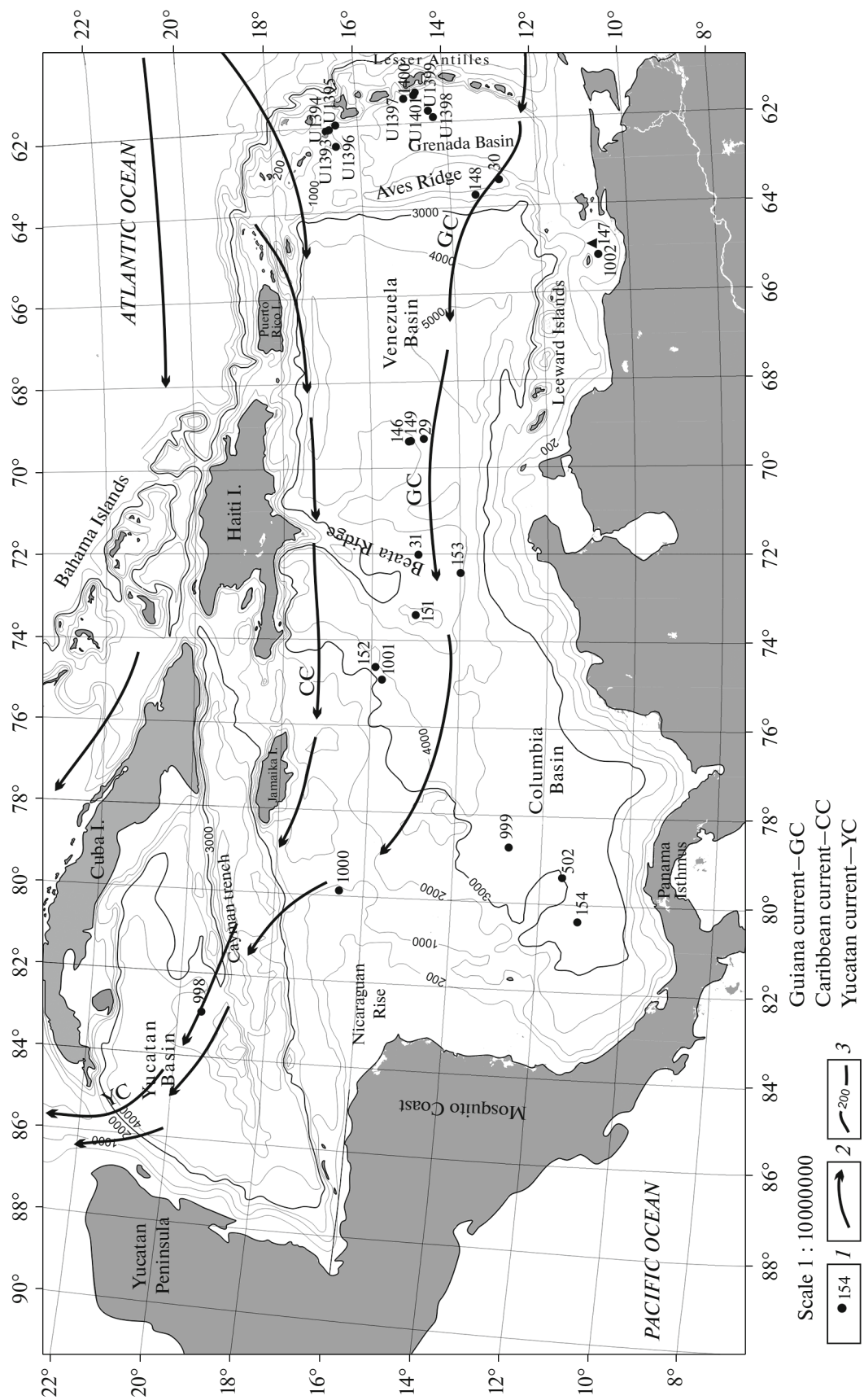

Fig. 1. Position of deep-sea drilling holes in the Caribbean Sea. Symbols: (*1*) deep-sea drilling holes; (*2*) surface currents ((GC) Guiana Current; (CC) Caribbean Current; (YC) Yucatan Current (Sukhovei et al., 1980); (*3*) isobaths (m). Filled triangles show the position of the Cariaco basin.

nutrients required for plankton development cannot penetrate into the Caribbean Sea from the Atlantic Ocean through shallow straits connecting the basins. This explains the low primary production of the studied sea. Only in the extreme southeast, the values of annual production reach up to 180–250 g C/m^2/year in the influence zones of the Orinoco and Magdalena river runoff and Venezuela upwelling (O'Reilly and Sherman, 2016).

Geomorphologically, the deep-water floor of the Caribbean Sea is represented by an alternation of submarine rises and ridges, on the one hand, and deep-water basins, on the other. From the east westward, the seafloor topography comprises the Grenada Basin, the Aves Ridge, the Venezuela Basin, the Beata Ridge, the Columbia Basin, the Nicaraguan Rise, the deep-water Cayman Trench (maximum water depth of 7686 m)–Cayman Ridge tectonic pair, and the Yucatan Basin (Fig. 1). The floor depth of the deep-water basins is usually over 4000 m (reaching even 5000 m in the Venezuela Basin), while the crests of submarine ridges are located at a water depth of approximately 1500 m. The Nicaraguan Rise is the largest structure of the continental margin.

The main sources of the lithogenic (terrigenous, volcanogenic, and volcano-terrigenous) flux are the Windward Islands of the Lesser Antilles, which were a center of the volcanotectonic activity of the Pliocene–Quaternary island arc. Its additional sources are solid runoff of the Orinoco River, which is transferred westward by the coastal Guinea Current, and Magdalena River, which runs through Columbia and represents the largest river of the basin (1500 km long). Some sediment influx is also provided by the wave abrasion of the South and Central America coasts.

It is shown in the map of the surface bottom sediments of the Caribbean Sea (Melnik, 1989–1990) that the terrigenous sediments (mainly, sands) related to the river fans and coastal abrasion are accumulated within a narrow band on the southern shelf of the basin. Other shelves are mainly covered by coral reefs and biogenic–detrital carbonate sands (consisting of fragments of corals, mollusks, calcareous algae, echinoderms, and others). Low-carbonate terrigenous sediments (up to 30% $CaCO_3$) surround the Lesser Antilles and are developed in the southeastern Caribbean Sea, in particular, in the southern part of the Aves Ridge. To the north and west, they are replaced by carbonate (30–50% $CaCO_3$) sediments extending westward approximately up to the median line of the Venezuela Basin. Thereby, the submarine rises and ridges are covered by the coarser grained sediments (mainly, fine silty ooze), while finer, essentially pelitic sediments are developed in basins. The remained (western) part of the sea is practically completely occupied by high-carbonate (>50% $CaCO_3$) sediments, which, as carbonate deposits, show grain-size differentiation. There are also ubiquitous volcanic ashes rimming the Lesser Antilles.

FACTUAL MATERIAL

The considered region was spanned by four deep-sea drilling Leg: DSDP cruises 4 (Bader et al., 1970) and 15 (Edgar, Saunders et al., 1973), ODP Leg 165 (Sigurdsson et al., 1997), and IODP Leg 340 (Le Friant et al., 2013). The position of holes is shown in Fig. 1. Our considerations are based on lithological, stratigraphic, and physical data on the Pleistocene sediments taken from these reports.

Isobaths shown in Fig. 1 are from the General Bathymetric Chart of the World Ocean (www.gebco.org) published in 2004.

RESULTS

The factual material (Fig. 1) and lithological-facies (with isopachs) maps were compiled in the transverse azimuthal equal-area projection on a scale 1 : 10000000 for two age sections: Neo- and Eopleistocene (Figs. 2 and 3).

Neopleistocene. The Neopleistocene lithological-facies map (Fig. 2) shows the distribution of main sediment types. The Neopleistocene facies structure is similar to the present-day one. The duration of the Neopleistocene also imparts vertical component.

Thus, the Windward Islands from the west, in the Grenada Basin are rimmed by a band of alternating hemipelagic clays, carbonate–volcanogenic (in some holes, volcanogenic) turbidites, and volcanic ashes. This sequence frequently comprises submarine landslides. The Neopleistocene sediments of the Aves Ridge are represented by alternating foraminiferal clays and hemipelagic clays. In the Neopleistocene, a homogenous sequence of hemipelagic clays occupied the most part of the Venezuela Basin floor and even southern shelf. Further westward, the abyssal floor is covered by the superlarge carbonate field (30–70% $CaCO_3$), which is made up of foraminiferal–coccolithic clays in the western part of the Venezuela Basin and partially, on the Beata Ridge, and westerly, of nanoclays. The western part of the Yucatan Basin floor in the Neopleistocene accumulated coccolithic ooze (nano-ooze) with $CaCO_3$ content more than 70%. The eastern half of the Nicaraguan Rise and significant part of the continental slope of the Yucatan Peninsula were covered by alternating nano-ooze and coccolithic ooze. Carbonate–detrital sediments are widespread on shoalings around the Leeward Islands and carbonate shelves of the Greater Antilles, Central America, and Yucatan. Terrigenous sands were accumulated in the southern coastal areas, being restricted to the influence zones of large river runoffs. The shelf Cariaco basin is filled with organic-rich fine mud.

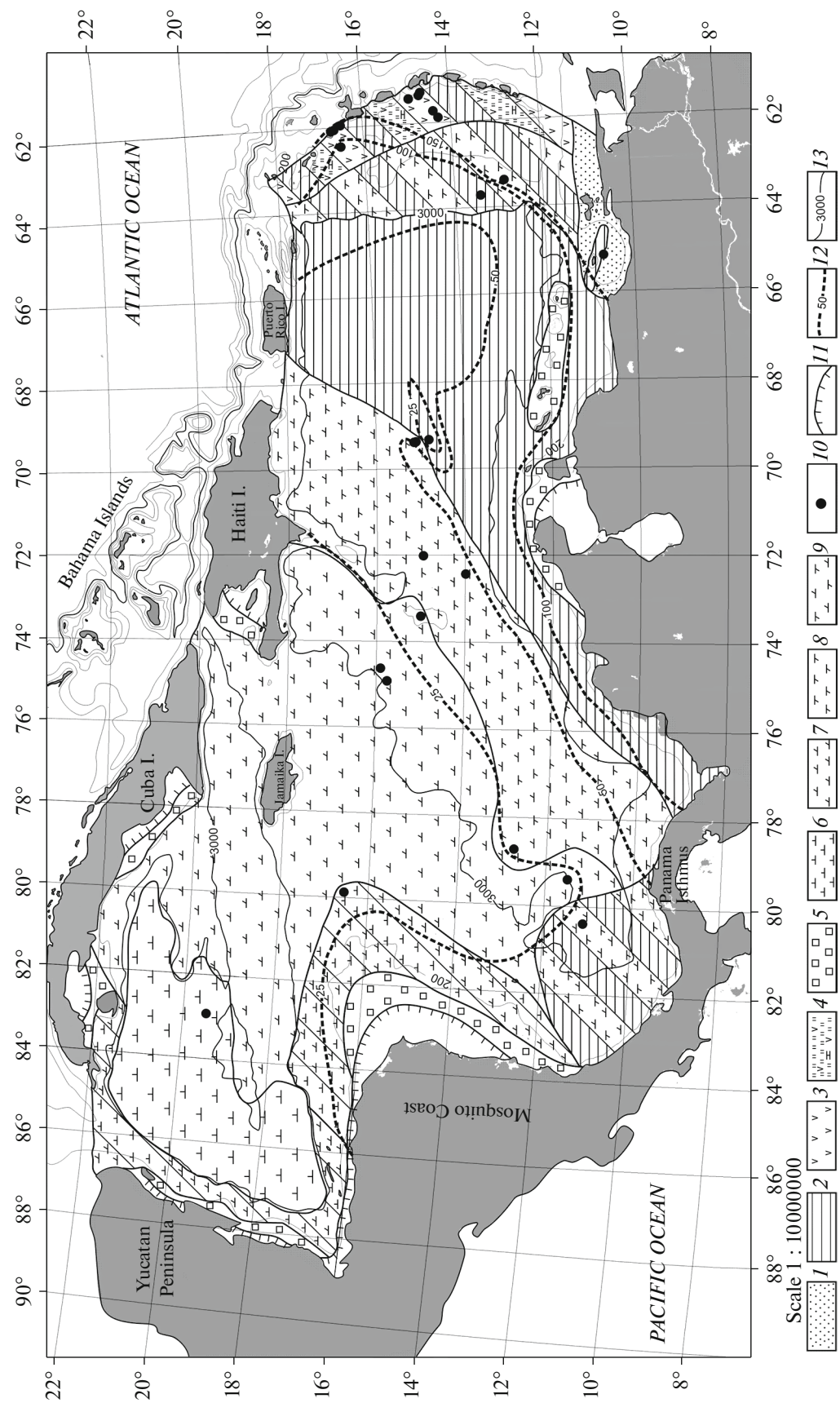

Fig. 2. Neopleistocene lithological-facies map. Symbols: (*1*) terrigenous sands; (*2*) hemipelagic clays; (*3*) volcanic ash; (*4*) carbonate–volcanogenic turbidites; (*5*) biogenic–detrital carbonate sediments; (*6*) nano-ooze; (*7*) nanoclays; (*8*) foraminiferal clays; (*9*) nanoforaminiferal clays; (*10*) deep-sea drilling holes; (*11*) coastal line; (*12*) isopachs (m); (*13*) isobaths (m). Diagonal lines mean alternation.

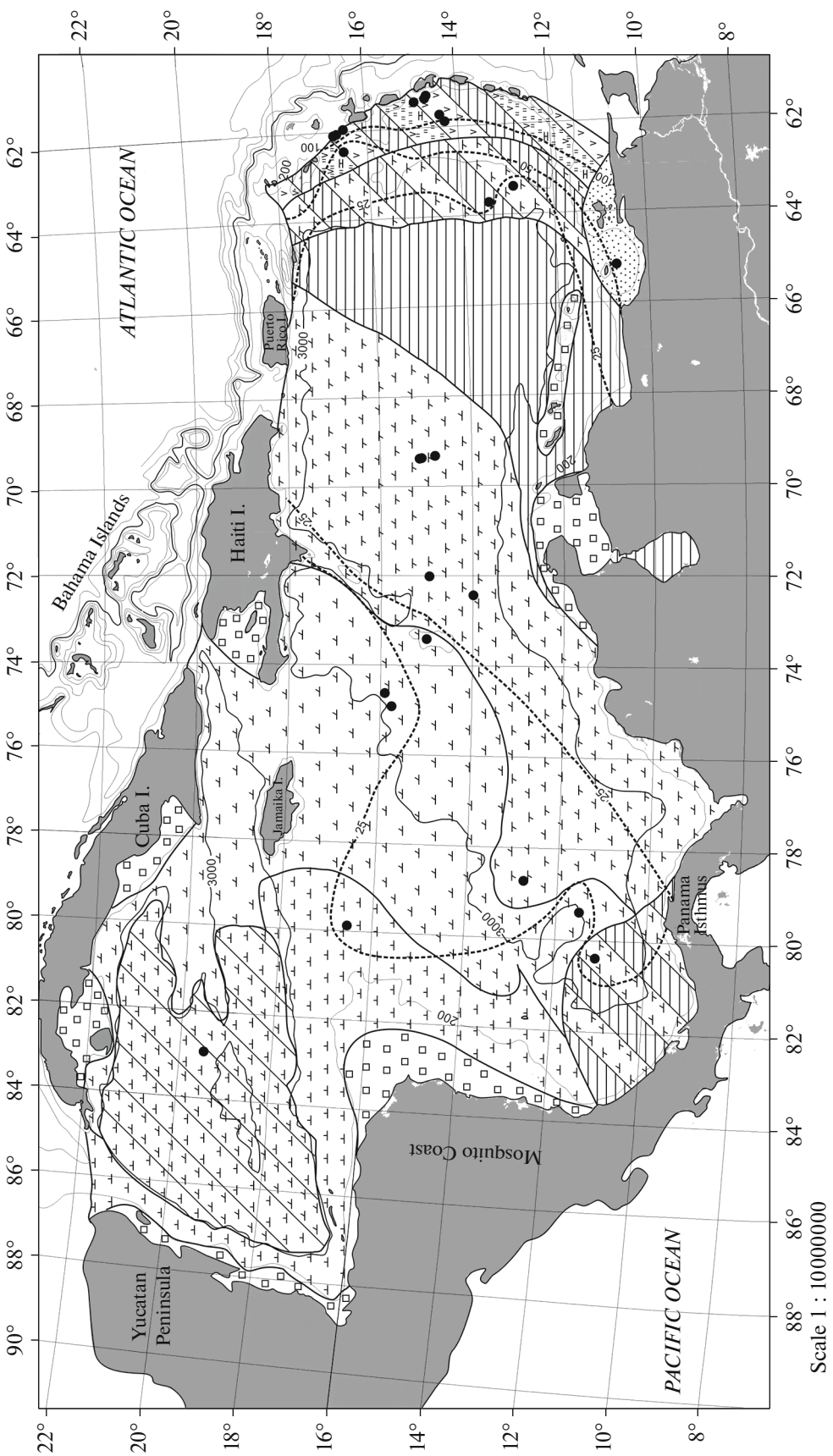

Fig. 3. Eopleistocene lithological-facies map. For symbols, see Fig. 2.

Table 1. Areas (S, thou. km^2) and volumes (V, thou. km^3) of the Neopleistocene deposits in the Caribbean Sea

Biogenic-detrital carbonate sediments		Nano-ooze		Nanoclays		Hemipelagic clays		Nano-foraminiferal clays		Terrigenous sands	
S	V	S	V	S	V	S	V	S	V	S	V
112.7	2.2	202.0	3.0	728.8	16.8	467.0	30.8	405.4	18.03	30.5	5.1

Alternation				Alternation				Alternation			
S	Nano-ooze	Nanoclays	ΣV	S	Hemipelagic clays	Nano-foraminiferal clays	ΣV	S	Hemipelagic clays	Foraminiferal clays	ΣV
	V	V			V	V			V	V	
211.5	4.3	1.5	5.8	112.0	0.8	3.4	4.2	123.6	10.4	2.6	13.0

Alternation					Total area of all sediments	Total volume of all sediments
S	Ash	Hemipelagic clays	Carbonate-volcanogenic turbidites	ΣV	ΣS	ΣV
	V	V	V			
78.1	0.6	8.5	3.8	12.9	2471.6	111.83

The thickness distribution of the Neopleistocene sediments (Fig. 2) with confidence indicates that at that time, as in the modern epoch, the main sources of lithogenic matter were Windward Islands, with subordinate contribution from the South and Central America coasts. The thickness of the Neopleistocene deposits near the Windward Islands frequently exceeds a few hundreds of meters. Westward, it rapidly decreases to 100 m. The 50- and 25-m isopachs are located approximately parallel and closely to 100-m isopach and extended further westward. The thickness of the Neopleistocene sediments over the most part of the studied basin is no more than 25 m thick.

Results of processing of the considered map (Fig. 2) using A.B. Ronov's volumetric method are shown in Table 1. The Neopleistocene sediments span an area of 2471.6 thou. km^2 and their total volume is 111.8 thou. km^3. Nanoclays (728.8 thou. km^2) are the first most abundant sediments. They are followed by hemipelagic clays (467.0 thou. km^2), nanoforaminiferal clays (405.4 thou. km^2), alternating nano-ooze and nanoclays (211.5 thou. km^2), nano-ooze (202.0 thou. km^2), alternating hemipelagic clays and foraminiferal clays (123.6 thou. km^2), biogenic–detrital carbonate sediments (112.7 thou. km^2), alternating hemipelagic clays and nanoforaminiferal clays (112.0 thou. km^2), and other types of sediments and their alternations, which occupy no more than dozens of thou. km^2.

By volume (Table 3), Neopleistocene sediments are arranged in the following series (in decreasing order): hemipelagic clays—45.05%, nanoforaminiferal clays—19.36%, nanoclays—16.32%, nano-ooze—6.51%, terrigenous sands—4.55%, carbonate–volcanogenic turbidites—3.39%, foraminiferal clays—2.32%, biogenic–detrital carbonate sediments—1.96%, and volcanic ash—0.54%.

Using formula published in (Levitan et al., 2013), the volumes of natural sediments were recalculated for dry sediment mass expressed in 10^{18} g. Obtained series of the dry sediment mass (in decreasing order) is as follows (Table 4): hemipelagic clays (43.94), nanoforaminiferal clays (17.36), nanoclays (15.52), nano-ooze (6.42), terrigenous sands (5.97), carbonate–terrigenous turbidites (5.19), biogenic-detrital carbonate sediments (2.24), foraminiferal clays (1.66), and volcanic ash (0.61).

The accumulation rate in the Neopleistocene expressed in 10^{18} g/Ma (see Table 4) in decreasing order varies from 55.62 for hemipelagic clays, 21.97 for nanoforaminiferal clays, 19.65 for nanoclays, up to 2.10 for foraminiferal clays and 0.77 for volcanic ash.

Eopleistocene. In the east of the Caribbean Sea (the Grenada Basin and Eaves Ridge), the Eopleistocene facies structure is practically identical to the Neopleistocene one (Fig. 3). However, the distribution area of hemipelagic clays in the Venezuela Basin significantly decreased. The accumulation area of the foraminiferal–coccolithic clays and nanoclays significantly increased in the central part of the basin and further westward, respectively. Most part of the Yucatan Basin is occupied by the alternation of nano-ooze and nanoclays, while the area of high-carbonate nano-ooze was shifted in the shallower water zone on the Nicaraguan Rise. Shelves accumulated the same sediments as in the Neopleistocene. However, due to the higher sea level, the area of the biogenic-detrital carbonate sedi-

Table 2. Area (S, thou km^2) and volumes (V, thou km^3) of the Eopleistocene deposits in the Caribbean Sea

Terrigenous sands		Biogenic-detrital carbonate sediments		Hemipelagic clays		Nanoforaminiferal clays		Nanoclays		Nano-ooze	
S	V	S	V	S	V	S	V	S	V	S	V
28.0	1.9	178.3	2.2	305.1	8.5	611.3	10.4	620.3	12.0	300.3	4.3

Alternation				Alternation				Alternation				
S	Nano-ooze	Nanoclays	ΣV	S	Hemipelagic clays	Nano-foraminiferal clays	ΣV	S	Volcanic ashes	Hemipelagic clays	Carbonate-volcan. turbidites	ΣV
	V	V			V	V			V	V	V	
288.0	2.7	0.9	3.6	101.3	0.4	1.4	1.8	142	0.4	2.4	5.1	7.9

Total areas of all sediments	Total volumes of all sediments
2574.6	52.6

Table 3. Areas (S, thou. km^2) and volumes (V, thou. km^3) of the Pleistocene deposits of the Caribbean Sea

Age	Terrigenous sand		Biogenic-detrital carbonate sediments		Hemipelagic clays		Nanoforaminiferal clays		Nanoclays		Nano-ooze	
	S	V	S	V	S	V	S	V	S	V	S	V
Neopleistocene	30.5	5.1	112.7	2.2	786.7	50.5	517.4	21.7	940.3	18.3	413.5	7.3
Eopleistocene	28.0	1.9	178.3	2.2	548.4	11.3	712.6	11.8	908.0	12.9	588.3	7.0

Age	Volcanic ash		Carbonate-volcan. turbidites		Foraminiferal clays	
	S	V	S	V	S	V
Neopleistocene	78.1	0.6	78.1	3.8	123.6	2.6
Eopleistocene	142.0	0.4	142.0	5.1	0	0

ments exceeded that of the Neopleistocene. Unfortunately, there are no accurate data on the development of the Eopleistocene coral reefs. Thus, compared to the Neopleistocene, the area of carbonate accumulation in the Eopleistocene was clearly higher, while the distribution of lithogenic sediments, significantly lower.

The thickness distribution of the Eopleistocene sediments (Fig. 3) retains a trend of their decreasing from the east westward, but a zone of low thicknesses (25–50 and less than 25 m) has much larger size than in the Neopleistocene. Its eastern boundary is significantly shifted eastward.

Processing of the considered map (Fig. 3) using A.B. Ronov's volumetric method is shown in Table 2. The Eopleistocene sediments occupy 2574.6 thou. km^2, while their total volume is 52.6 thou. km^3. Nanoclays (620.3 thou. km^2) are the first most abundant sediments. They are followed by nanoforaminiferal clays (611.3 thou. km^2), hemipelagic clays (305.1 thou. km^2), nano-ooze (300.3 thou. km^2), alternating nano-ooze and nanoclays (288.0 thou. km^2), biogenic–detrital carbonate sediments (178.3 thou. km^2), alternating volcanic ash, hemipelagic clays and carbonate–volcanogenic turbidites (142.0 thou. km^2), alternating hemipelagic clays and nanoforaminiferal clays (101.3 thou. km^2), and terrigenous sands (28.0 thou. km^2).

By volumes (Table 3), the Eopleistocene sediments form the following series (also in decreasing order): nanoclays—24.51%, nanoforaminiferal clays—22.42%, hemipelagic clays—21.47%, nano-ooze—13.3%, and carbonate–volcanogenic turbidites—9.69%. Volumes of other types of sediments account for less than 5% of the total volume of Eopleistocene sediments.

The calculated series of dry sediment mass expressed in 10^{18} g is as follows (Table 4): nanoclays—11.39, hemipelagic clays—10.85, nano-foraminiferal clays—10.71, carbonate–volcanogenic turbidites—6.96, and nano-ooze—6.58. Masses of other sediments account for less than 3.00×10^{18} g. Since the duration of Eopleistocene accepted in this work is 1.0 Ma, the accumulation rate of Eopleistocene sediments expressed in 10^{18} g/Ma is arranged in the same series (Table 4).

Table 4. Mass of dry sediment (M, 10^{18} g) and accumulation rate (I, 10^{18} g/Ma) of Pleistocene sediments of the Caribbean Sea

Age	Terrigenous sands		Biogenic-detrital carbonate sediments		Hemipelagic clays		Nanoforaminiferal clays		Nanoclays		Nano-ooze	
	M	I	M	I	M	I	M	I	M	I	M	I
Neopleistocene	5.97	7.56	2.24	2.84	43.94	55.62	17.36	21.97	15.52	19.65	6.42	8.13
Eopleistocene	2.22	2.22	2.24	2.24	10.85	10.85	10.71	10.71	11.39	11.39	6.58	6.58

Age	Volcanic ash		Carbonate–volcan. turbidites		Foraminiferal clays	
	M	I	M	I	M	I
Neopleistocene	0.61	0.77	5.19	6.57	1.66	2.10
Eopleistocene	0.41	0.41	6.96	6.96	0	0

Dividing the Neopleistocene accumulation rate by the Eopleistocene one ($I\ Q_{2+3}/I_1$) yields the following proportions for major sediment types: hemipelagic clays 5.13, foraminiferal clays—2.05, nanoclays—1.73, nano-ooze—1.24, terrigenous sands—3.41, carbonate–volcanogenic turbidites—0.94, biogenic–clastic carbonate deposits—1.27, volcanic ash—1.88. Thus, the obtained data indicate that the accumulation of terrigenous sediments in the Neopleistocene was more intense than in the Eopleistocene, whereas the accumulation of high-carbonate and volcanogenic rocks was less intense, and the accumulation of carbonate sediments (30–70% $CaCO_3$), was intermediate.

DISCUSSION

The comparison of the Eopleistocene (Fig. 3) and Neopleistocene (Fig. 2) lithological-facies maps and maps of the surface sediments of the Caribbean Sea (Emel'yanov et al., 1989–1990) revealed their similar facies structure, which have preserved during Quaternary. Lithogenic fluxes were supplied in the sedimentation basin from the east and southeast, the primary production remained sufficiently low, and carbonates were accumulated (mainly at the expense of plankton) in areas where carbonate fluxes became equal to or exceeded lithogenic fluxes, i.e., mainly in the western Caribbean Sea.

Thereby, the Quaternary sedimentation demonstrates a definite evolution. We believe that a clear increase of lithogenic fluxes is explained by the neotectonic activity of the Lesser Antilles and, to lesser extent, by their volcanic activity. The products of volcanic explosions were accumulated by aeolian activity and currents mainly in the proximity to sources. In particular, the interlayers and even units of volcanic ashes are abundant in the sedimentary cover of the Grenada Basin. Volcanogenic–terrigenous flux was mainly provided by along-slope turbid flows and submarine landslides, and, to lesser extent, by surface currents to the west. Compared to the Windward Islands, the neotectonic activity of the Leeward Islands, Greater Antilles, and Panama Isthmus was insignificant.

Some intensification of carbonate accumulation in the Pleistocene is mainly explained by increasing production of carbonate-concentrating organisms and associated increasing the carbonate compensation depth (CCD). By the way, an increase of CCD during Late Cenozoic, in particular, from the Pliocene to the Pleistocene, was noted during the first deep-sea drilling cruises in the Caribbean Sea (Hay, 1970). Note that an increase of carbonate sedimentation rate during Pleistocene is in conflict with our data on the Atlantic pelagic sediments (Levitan and Gelvi, 2016). A decrease of carbonate accumulation in the pelagic zone in the Neopleistocene compared to the Eopleistocene is explained by a sharply increased production of bottom and deep Antarctic waters during the Middle Pleistocene transition (Levitan and Gelvi, 2016). These waters are not favorable for carbonate precipitation owing to their extremely low temperatures and peculiar acid–basic properties (Flower, 1999). It was noted above that such waters did not enter the Caribbean Sea due to the shallow depths of straits linking it with the Atlantic Ocean.

At the same time, a definite similarity in the trends of accumulation rates of lithogenic and carbonate material in the Caribbean Sea during Pleistocene likely indicates their relationships: a simultaneous influx of the denudation products of the Lesser Antilles and dissolved nutrients as chemical weathering products during the neotectonic uplift of the Lesser Antilles.

FUNDING

This paper was partially supported by the Russian Foundation for Basic Research (project no. 17-05-00157) and by the Presidium of the Russian Academy of Sciences (project no. 20). This work was made in the framework of the State Task no. 0137-2016-0008.

REFERENCES

R. G. Bader, et al., Init. Repts. DSDP **4**, (1970). N. T. Edgar, J. B. Saunders, et al., Init. Repts. DSDP **15**, (1973).

B. Flower, "Cenozoic deep-sea temperatures and polar glaciation: the oxygen isotope record," Terra Antarct. Rep. **3**, 27–42 (1999).

F. M. Gradstein, J. G. Ogg, A. G. Smith, et al., *A Geologic Time Scale 2004* (Cambridge Univ. Press, 2004).

W. W. Hay, "Calcium carbonate compensation," Init. Repts. DSDP **4**, 672–673 (1970).

Le Friant, A. O. Ishizuka, N. A. Stroncik, et al., Proc. IODP, Init. Repts., 340, (2013).

M. A. Levitan and T. N. Gelvi "Quantitative parameters of pelagic Pleistocene sedimentation in the Atlantic," Geochem. Int. **54** (12), 1091–1103 (2016).

M. A. Levitan, A. N. Balukhovsky, T. A. Antonova, and T. N. Gelvi, "Quantitative parameters of Pleistocene pelagic sedimentation in the Pacific Ocean," Geochem. Int. **51** (5), 345–352 (2013).

M. A. Levitan, T. N. Gelvi, K. V. Syromyatnikov, and K. D. Chekan "Facies structure and quantitative parameters of Pleistocene sediments of the Bering Sea," Geochem. Int. **56** (4), 304–317 (2018).

M. A. Levitan, T. A. Antonova, and A. V. Koltsova, "Facies structure and quantitative parameters of Pleistocene sediments from the East Australian continental margin," Geochem. Int. **57**(6), 698–708 (2019).

M. A. Levitan, T. N. Gelvi and L. G. Domaratskaya "Facies structure and quantitative parameters of Pleistocene sedimentation on the deep–sea floor of the southern Pacific Ocean and in the Scotia Sea, Lithol. Miner. Resour. **55** (5), 327–337 (2020).

V. I. Melnik, Caribbean Sea. Types of Bottom Sediments (1989–1990). International Geological–Geophysical Atlas of the Atlantic Ocean, Ed. by G. B. Udintsev, (MOK (UNESCO), Mingeo SSSR, GUGK SSSR, Moscow, 1990) [in Russian].

I. O. Murdmaa, Oceanic Facies (Nauka, Moscow, 1987) [in Russian].

J. O'Reilly, and K. Sherman, "Primary productivity patterns and trends," In: *IOC–UNESCO and UNEP Large Ecosystems: Status and Trends* (United Nations Environment Programme, Nairobi, 2016), pp. 91–99.

A. B. Ronov, *History of Sedimentation and Oscillatory Motions in the European USSR: Volumetric Method Data*, (Geofiz. Inst. AN SSSR. Moscow, 1949), Vol. 3 [in Russian].

H. Sigurdsson, R. M. Leckie, G. D. Acton, et al., Proc. ODP, Init. Repts. 165, (1997).

N. M. Strakhov, "Comparative–lithological direction and its nearest tasks," Byul. Mosk. O-va Ispyt. Prir., Otd. Geol. **20** (3/4), 34–48 (1945).

V. F. Sukhovei, G. K. Korotaev, and N. B. Shapiro, *Hydrology of the Caribbean sea and Mexican Bay* (Gidrometeoizdat, Leningrad, 1980) (1980) [in Russian]

www.gebco.org (2004).

Translated by M. Bogina